

Modern Control Laws for an Articulated Robotic Arm

Modeling and Simulation

Jamshed Iqbal

Department of Electrical and Electronics Engineering, University of Jeddah, Saudi Arabia

Department of Electrical Engineering, FAST National University, Islamabad, Pakistan

jmiqbal@uj.edu.sa

Abstract—The robotic manipulator has become an integral component of modern industrial automation. The current paper deals with the mathematical modeling and non-linear control of this manipulator. DH-parameters are used to derive kinematic model while the dynamics is based on Euler-Lagrange equation. Two modern control strategies, H^∞ and model predictive control (MPC), are investigated to develop the control laws. For an optimal performance, the controllers have been fine-tuned through a simulation conducted in MATLAB/Simulink environment. The designed control laws are subjected to various inputs and tested for effectiveness in transient parameters like settling time and overshoot as well as steady state error. Simulation results confirm the effectiveness of the developed controllers by precisely tracking the reference motion trajectories.

Keywords—non-linear control; robotic arm manipulator; mechatronics; DH-parameters; Euler-Lagrange equation

I. INTRODUCTION

Robots are considered key elements in automation, thus their application horizon is increasing [1]. Autonomy and intelligence in robots is primarily caused by the advancements in technology and research in domains like modeling, design, control and artificial intelligence (AI) [2]. Modeling and simulation in different scientific domains is gaining enormous interest among the scientific community in order to develop in-depth understanding of real-world applications. Study and modeling of an anthropomorphic system may help the better understanding of general human biomechanics and may also lead to formulating control laws of the actual biological agent. The basis of developing the control system for a robotic manipulator is the feedback loop, which plays a pivotal role to dampen the uncertainties. The control system neutralizes numerous disturbances and uncertainties in the plant. The solution to the control problem involves defining input signals like torque or actuator input voltage to achieve the desired behavior. The controller must be capable of handling the effects of nonlinearities, dynamic coupling and complexity. Trivial strategies based on linear control laws are not able to handle the above mentioned issues [3]. Thus, implementation of nonlinear control laws has been presented [4-7]. To meet the performance requirements to control multi-degree of freedom (DOF) robotic manipulators, nonlinear control based on sliding mode control (SMC) [8, 9], computed torque control (CTC),

H^∞ and model predictive control (MPC) [10] have been reported.

MPC is an optimal control technique which predicts the future behavior of the system based on current states and responses. To ensure better tracking performance in constrained environment, an online process is utilized to compute future values. The optimized control signal is then formulated considering both prediction results and past behavior. An in-depth review of MPC based control strategies has been presented in [11]. Authors in [12] used MPC for position and force control of a human arm like a seven DOF robotics manipulator. In [13], a real-time computation method for MPC has been presented, which introduced a mapping of offline approximation approach in neural networks (NN). The proposed technique has been implemented on a low cost field programmable gate array (FPGA) to show its less hardware and computational time requirements. A comparison of MPC with the proportional integral derivative (PID) and CTC has been presented in [14]. Authors in [15] have proposed NN based MPC and PID law to control the vibration and position of 2-link flexible arm. H^∞ control law provides system robustness and high performance in spite of uncertainties and disturbances. In this control law, it is assumed that all the system states and disturbances can be sent as feedback to create a close loop system. Authors in [16] presented feedback control of a linearized model of a selective compliance assembly robot arm (SCARA) based on H^∞ control. In [17], authors suggested discrete time dynamical method as a solution of the H^∞ control problem. A state-space H^∞ solution using the Riccati equation has been proposed in [18]. H^∞ framework has been used in [19] to solve the control and management problem of tradeoffs in the specifications.

This paper presents the design of H^∞ and MPC control laws for a six DOF robotic arm where links and joints are serially connected. The formulation of the control laws is based on the derived kinematics and dynamics of the robotic arm. The efficacy of both control strategies has been demonstrated through tracking results for various inputs.

II. MATHEMATICAL MODEL OF THE ROBOTIC ARM

Robotic manipulator ED7220C is a commercial robot developed for academic purposes. This anthropomorphic arm is

used for modeling and control in the present work. The end-effector is a gripper. All joints have a single DOF except the wrist. The wrist can move in roll and pitch planes. Specifications of the robotic arm are presented in [20].

A. Kinematic Models

Kinematic modeling involves the joints and the end-effector position without considering the associated forces. It provides the position and orientation of end-effector based on robot joints' angular position. In the present research, DH parameter based approach has been used to derive the kinematics of the manipulator. The axis assignment is shown in Figure 1 and the resulting DH parameters are expressed in Table I.

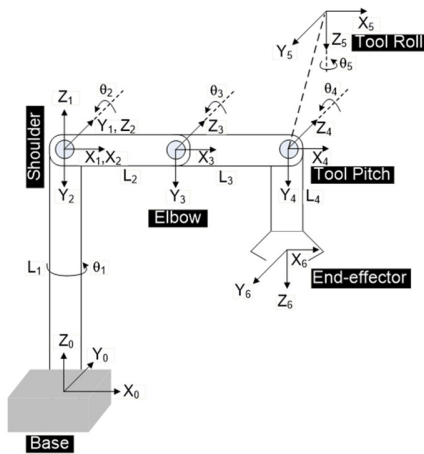


Fig. 1. Kinematic representation of the arm showing assignment of frames on various joints

TABLE I. DENAVIT-HARTENBERG (DH) PARAMETERS

Parameter	Symbol	Joint (i)					
		1	2	3	4	5	6
Link twist	α_{i-1}	0	-90°	0	0	-90°	0
Link length	a_{i-1}	0	0	l_2	l_3	0	0
Joint angle	θ_i	θ_1	θ_2	θ_3	θ_4	θ_5	0
Joint distance	d_i	l_1	0	0	0	0	l_4

The transformation matrices, calculated through DH-parameters presented in Table I, for each link are given in (1), while the overall transformation is computed as given in (2):

$$\begin{aligned}
 {}^0_1T &= \begin{bmatrix} c_1 & -s_1 & 0 & 0 \\ s_1 & c_1 & 0 & 0 \\ 0 & 0 & 1 & l_1 \\ 0 & 0 & 0 & 1 \end{bmatrix} & {}^1_2T &= \begin{bmatrix} c_2 & -s_2 & 0 & 0 \\ 0 & 0 & 1 & 0 \\ -s_2 & -c_2 & 0 & 0 \\ 0 & 0 & 0 & 1 \end{bmatrix} \\
 {}^2_3T &= \begin{bmatrix} c_3 & -s_3 & 0 & l_2 \\ s_3 & c_3 & 0 & 0 \\ 0 & 0 & 1 & 0 \\ 0 & 0 & 0 & 1 \end{bmatrix} & {}^3_4T &= \begin{bmatrix} c_4 & -s_4 & 0 & l_3 \\ s_4 & c_4 & 0 & 0 \\ 0 & 0 & 1 & 0 \\ 0 & 0 & 0 & 1 \end{bmatrix} \\
 {}^4_5T &= \begin{bmatrix} c_5 & -s_5 & 0 & 0 \\ 0 & 0 & 1 & 0 \\ -s_5 & -c_5 & 0 & 0 \\ 0 & 0 & 0 & 1 \end{bmatrix} & {}^5_6T &= \begin{bmatrix} 1 & 0 & 0 & 0 \\ 0 & 1 & 0 & 0 \\ 0 & 0 & 1 & l_4 \\ 0 & 0 & 0 & 1 \end{bmatrix} \\
 {}^0_6T &= {}^0_1T {}^1_2T {}^2_3T {}^3_4T {}^4_5T {}^5_6T \\
 &= \begin{bmatrix} c_1c_{234}c_5 + s_1s_5 & -c_1c_{234}s_5 + s_1c_5 & -c_1s_{234} & c_1A \\ s_1c_{234}c_5 - c_1s_5 & -s_1c_{234}s_5 - c_1c_5 & -s_1s_{234} & s_1A \\ -s_{234}c_5 & s_{234}s_5 & -c_{234} & B \\ 0 & 0 & 0 & 1 \end{bmatrix}
 \end{aligned}
 \tag{1}$$

and the nomenclature used is: $s_{ab}=\sin(a+b)$, $s_{abc}=\sin(a+b+c)$, $c_{ab}=\cos(a+b)$, and $c_{abc}=\cos(a+b+c)$.

Given the required position and orientation of the tool, the transformation matrix presented in (2) is used to determine the corresponding joint angles. The computed joint angle positions are achieved through the controller which generates the appropriate signals for the DC motors but this requires the dynamic model presented below.

B. Dynamic Model

The dynamic model of the robotic arm gives information of torque and other forces resulting in the motion of the robot. The dynamic model can be formulated using various methods including recursive Lagrange, recursive Newton-Euler and Euler-Lagrange. The dynamic model derived here uses the Euler-Lagrange equations. This is the most commonly followed approach due to its simplicity and compact description. The nomenclature for the deriving dynamics of the arm is presented in Table II.

TABLE II. NOMENCLATURE FOR DYNAMIC MODEL

Symbol	Remarks
m_i	Mass of link i
i_cP	Position of center of mass (CoM) of link i
${}^i_i\omega$	Angular velocity of link i with reference to its frame
v_{c_i}	Linear velocity of link i w.r.t. its CoM
k_T	Total kinetic energy related to each link
u_T	Total potential energy related to each link
u_{refi}	Potential energy reference
i_iI	Inertia tensor of link i with reference to its frame
g	Acceleration of gravity

The potential and kinetic energy of each link of the arm have been computed using (3-4) respectively:

$$u_i = -m_i g^T {}^i_cP + u_{refi} \tag{3}$$

$$k_i = \frac{1}{2} m_i v_{c_i}^T v_{c_i} + \frac{1}{2} {}^i_i\omega^T I_i {}^i_i\omega \tag{4}$$

Lagrangian has been calculated by the difference of these energies of the complete system. Torque corresponding to each link is determined by the partial differentiation of Lagrangian w.r.t q and \dot{q} as given in (5):

$$L = k_T - u_T, \quad \tau = \frac{d}{dt} \frac{\partial L}{\partial \dot{q}} - \frac{\partial L}{\partial q} \tag{5}$$

The resulting torque is given in (6):

$$\tau = M(q, \dot{q})\ddot{q} + g(q) + V(q, \dot{q}) \tag{6}$$

where τ is the 4×1 torque vector applied to the robot's joints. $g(q)$, $V(q, \dot{q})$ and $M(q, \dot{q})$ are respectively the 4×1 vector of gravitational force, the 4×1 vector of Coriolis centrifugal force and the 4×4 inertia matrix. \ddot{q} , \dot{q} and q are 4×1 vectors for angular acceleration, angular velocity and angular position. For complete derivation of system dynamics, see [20].

III. THE CONTROLLER DESIGN

A. MPC Based Controller

The key concept behind the design of the MPC law is to consider a discrete-time model of a system and to formulate an

optimization problem which is solved based on an objective cost function. Consider a plant in discrete-time representation (7)-(8) where the number of inputs is m , the number of outputs is q and the number of states is n_l .

$$x(k+1) = Ax(k) + Bu(k) \tag{7}$$

$$y(k) = Cx(k) \tag{8}$$

where u is the control input vector, x is the state vector, and y is the output vector. A is a square matrix termed as state matrix while B is the input matrix. A and B are properties of the system and are based on the system's elements and structure. C is the output matrix which depends on the particular choice of output variables. The optimal control signal can be written as in (9):

$$\Delta U = (\Phi^T \Phi + \bar{R})^{-1} (\Phi^T R_s - \Phi^T F x(k_i)) \tag{9}$$

where,

$$\Phi = \begin{bmatrix} CB & 0 & 0 & \dots & 0 \\ CAB & CB & 0 & \dots & 0 \\ \dots & \dots & \dots & \dots & \dots \\ CA^{N_p-1}B & CA^{N_p-2}B & CA^{N_p-3}B & \dots & CA^{N_p-N_c}B \end{bmatrix}$$

N_p and N_c represent the number of samples used for prediction and the number of samples used for control respectively. Also,

$$F = \begin{bmatrix} CA \\ CA^2 \\ \dots \\ CA^{N_p} \end{bmatrix}$$

R_s in (9) is the set-point information and can be represented based on set-point signal r_{k_i} i.e.

$$R_s^T = [1 \ 1 \ \dots \ 1] r(k_i) = \bar{R} r(k_i)$$

The principle of receding horizon is employed in developing incremental optimal control, which gives rise to:

$$u(k) = \sum_1^k \Delta u(k_i)$$

$$\Delta u(k_i) = K_y r(k_i) - K_{mpc} x(k_i)$$

where

$$u(k) = \sum_1^k \Delta u(k_i)$$

$$K_{mpc} = \text{First row of } (\Phi^T \Phi + \bar{R})^{-1} (\Phi^T F)$$

$$K_y = \text{First element of } (\Phi^T \Phi + \bar{R})^{-1} (\Phi^T R_s)$$

In the present work, feedback linearization has been used to linearize the nonlinear system given in (6). The state feedback control law for linearization of the model is given in (10).

$$\tau = M(q)(u_c - \dot{q} - q) + g(q) + V(q, \dot{q}) \tag{10}$$

where u_c is given by receding horizon algorithm i.e.:

$$u_c(k) = \sum_1^k \Delta u_c(k_i), \Delta u_c(k_i) = K_y r(k_i) - K_{mpc} x(k_i)$$

Thus, a complete MPC law can be expressed as in (11):

$$\tau(k) = M(-\dot{q}(k) - q(k) + \sum_1^k \{K_y r(k_i) - K_{mpc} x(k_i)\}) + V + g \tag{11}$$

The developed law resides on matrices K_y and K_{mpc} . Their

values are based on number of samples N_p and N_c . Thus, the overall computation time depends on window sizes.

B. H^∞ Control Law

To design H^∞ control law, a minimization problem is formulated while considering stability, robustness and performance normalization. The minimization problem is solved using the infinitive norm for the feedback-loop transfer function matrix. Considering a linear plant, (12) gives the generalized state space model.

$$\begin{aligned} \dot{x}(t) &= Ax(t) + Bu(t) \\ y(t) &= Cx(t) + Du(t) \end{aligned} \tag{12}$$

where $x(t)$, $u(t)$ and $y(t)$ represent state vectors, control input and output respectively. D is a feed forward matrix or direct transmission matrix which is determined by the selected output variables. Considering a perturbed system with disturbance vector $w(t)$ and error vector $z(t)$, (13) represents the state space model while (14) gives the transfer function matrix.

$$\begin{aligned} \dot{x}(t) &= Ax(t) + B_1 w(t) + B_2 u(t) \\ y(t) &= C_2 x(t) + D_{21} w(t) + D_{22} u(t) \\ z(t) &= C_1 x(t) + D_{11} w(t) + D_{12} u(t) \end{aligned} \tag{13}$$

$$T(s) := \begin{bmatrix} A & \vdots & B_1 & B_2 \\ \dots & \dots & \dots & \dots \\ C_1 & \vdots & D_{11} & D_{12} \\ C_2 & \vdots & D_{21} & D_{22} \end{bmatrix} \tag{14}$$

H^∞ control law is designed using state feedback linearization approach based on (6). The developed control law is given in (15).

$$\tau = M(q)(u_c - \dot{q} - q) + g(q) + V(q, \dot{q}) \tag{15}$$

where u_c is the auxiliary control signal. After applying (15), appropriate values of weight coefficients W_u and W_p are respectively selected for the perturbation and input. The calculation of K is based on S over KS design approach and solution of the two Riccati equations, ensuring the stability of the system i.e.:

$$\min_{K \text{ stabilizing}} \left\| \begin{bmatrix} W_p(I + TK)^{-1} \\ W_u K(I + TK)^{-1} \end{bmatrix} \right\|_\infty < \gamma \tag{16}$$

K serves as an auxiliary control which gives the signals u_{ci} as output based on the input joint angles q_i . $u_c = [u_{c1} \ u_{c2} \ u_{c3} \ u_{c4}]^T$ can be calculated after all u_{ci} are known.

IV. SIMULATION RESULTS AND DISCUSSION

MATLAB/Simulink is used for simulation. S-functions are used for the plant and controller in simulation environment. A sampling time of 5ms is selected for controlling the modeled robotic manipulator.

A. MPC Simulation Results

The performance of MPC control law for different target trajectories is investigated. The investigation also includes the effect of the control horizon N_c and the prediction horizon N_p .

Keeping N_c constant while changing N_p and vice versa revealed the importance of both horizons in the controller design. It is observed that the response of the system is related with the size of the control window. The performance is enhanced when the size is increased. Tuning based on trial and error resulted in optimal values as $N_p = 100$ and $N_c = 20$. Figures 2 and 3 present the trajectory tracking results when the system is subjected to ramp and step inputs respectively. It can be inferred from the results that all the joints demonstrated identical response with different torques applied to the joints. Shoulder joint exhibited relatively higher torque requirements in comparison with wrist, elbow and waist joints.

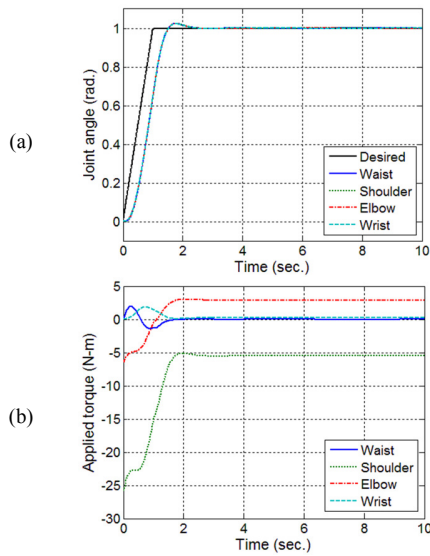


Fig. 2. Ramp response: (a) Trajectory tracking, (b) Corresponding torques

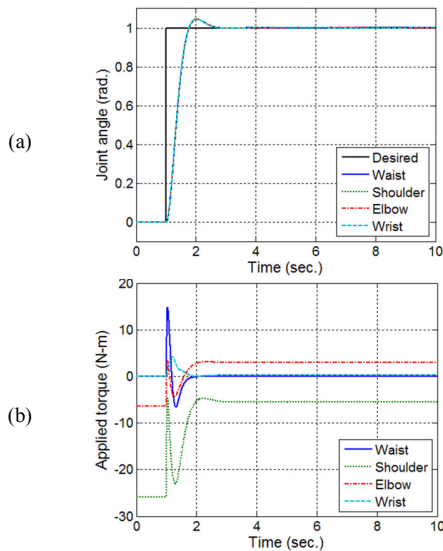


Fig. 3. Step response: (a) Trajectory tracking, (b) Corresponding torques

B. H^∞ Simulation Results

The weight functions have significant effect on the performance of the designed control law. In the present

research, the weight functions have been selected based on the guideline reported in [21]. The selected weight functions are given in (17):

$$W_p(s) = 0.95 \frac{s^2 + 1.5s + 1}{s^2 + 40s + 0.1} \text{ and } W_u(s) = 0.01 \tag{17}$$

The effect of changing W_u values on the developed controller is investigated. The results reveal that the selected value is a good choice. Weight functions (17) are used to plot ramp, step and sinusoidal responses of the system. Figures 4 and 5 present the tracking results of ramp and sinusoidal references. It is evident from the plots that all the joints of the robotic arm showed similar behavior. A delay is also observed in the controller's response for reference trajectories.

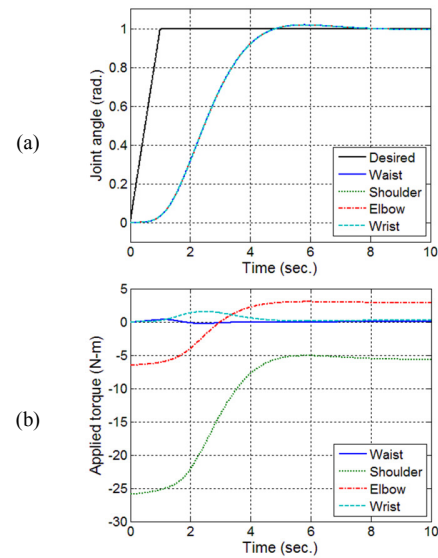


Fig. 4. Ramp response: (a) Trajectory tracking (b) Corresponding torques

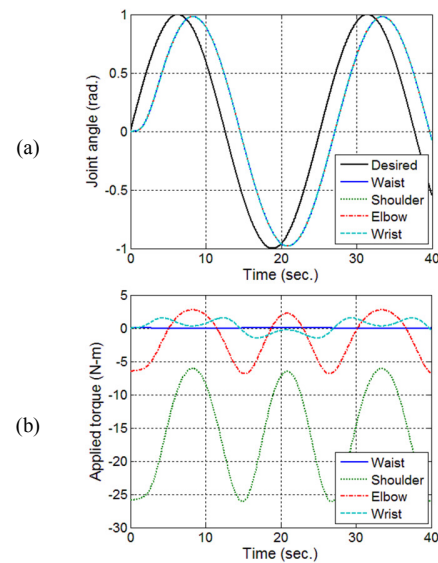


Fig. 5. Sinusoidal response: (a) Trajectory tracking, (b) Corresponding torques

The results obtained by MPC and H^∞ control laws are compared. The performance achieved by both controllers has been characterized w.r.t various parameters. Table III summarizes the comparative results based on step responses offered by both control strategies. For settling time, $\pm 5\%$ of the desired joint angle has been considered. It is pertinent to mention here that the given results are based on the selected gains and may vary with different gains selection.

TABLE III. COMPARATIVE PERFORMANCE

Parameter	Remarks	Control Strategy	
		H^∞	MPC
Rise time	t_r (sec)	4.305	0.77
Peak time	t_p (sec)	5.06	1.005
Settling time	t_s (sec)	3.68	0.68
Overshoot	%OS	1.9 %	4.5%

V. CONCLUSION

A model of a six DOF robotic arm is presented in this paper followed by the derivation of two modern control laws, MPC and H^∞ . Simulation results confirmed that both control laws offer adequate tracking performance. Comparative analysis of the performance achieved by both controllers reveals that MPC over performs H^∞ , on the expense of higher overshoot for controlling the robotic arm. The size of the prediction window can be increased to reduce overshoot in MPC response. In the future, it is planned to realize both control strategies on a real robotic platform. For this purpose, a custom platform named as AUTAREP (AUTonomous ARTICulated Robotic Educational Platform) has already been designed and fabricated. Also, it is planned to investigate the control performance when the robotic arm is subjected to disturbances and uncertainties. Moreover, application-oriented study to explore practical avenues of the proposed research is anticipated.

REFERENCES

- [1] J. Iqbal, R. U. Islam, S. Z. Abbas, A. A. Khan, S. A. Ajwad, "Automating industrial tasks through mechatronic systems—A review of robotics in industrial perspective", *Tehnicki Vjesnik*, Vol. 23, No. 3, pp. 917-924, 2016
- [2] S. G. Khan, G. Herrmann, M. Al Grafi, T. Pipe, C. Melhuish, "Compliance control and human-robot interaction: Part 1—Survey", *International Journal of Humanoid Robotics*, Vol. 11, No. 3, pp. 1430001-1430028, 2014
- [3] S. A. Ajwad, J. Iqbal, R. U. Islam, A. Alsheikhy, A. Almeshal, A. Mehmood, "Optimal and robust control of multi DOF robotic manipulator: Design and hardware realization", *Cybernetics and Systems*, Vol. 49, No. 1, pp. 77-93, 2018
- [4] I. Ahmad, A. Saaban, A. Ibrahim, M. Shahzad, "A research on the synchronization of two novel chaotic systems based on a nonlinear active control algorithm", *Engineering, Technology & Applied Science Research*, Vol. 5, No. 1, pp. 739-747, 2014
- [5] S. Irfan, A. Mehmood, M. T. Razzaq, J. Iqbal, "Advanced sliding mode control techniques for inverted pendulum: Modelling and simulation", *Engineering Science and Technology, an International Journal*, Vol. 21, pp. 753-759, 2018
- [6] W. Alam, A. Mehmood, K. Ali, U. Javaid, S. Alharbi, J. Iqbal, "Nonlinear control of a flexible joint robotic manipulator with experimental validation", *Strojinski Vestnik-Journal of Mechanical Engineering*, Vol. 64, No. 1, pp. 47-55, 2018
- [7] O. Khan, M. Pervaiz, E. Ahmad, J. Iqbal, "On the derivation of novel model and sophisticated control of flexible joint manipulator", *Revue*

- [8] Roumaine des Sciences Techniques-Serie Electrotechnique et Energetique, Vol. 62, No. 1, pp. 103-108, 2017
- [8] A. Rezoug, B. Tondou, M. Hamerlain, "Experimental study of nonsingular terminal sliding mode controller for robot arm actuated by pneumatic artificial muscles", *IFAC Proceedings*, Vol. 47, pp. 10113-10118, 2014
- [9] J. Iqbal, M. I. Ullah, A. A. Khan, M. Irfan, "Towards sophisticated control of robotic manipulators: An experimental study on a pseudo-industrial arm", *Strojinski Vestnik-Journal of Mechanical Engineering*, Vol. 61, No.7-8, pp. 465-470, 2015
- [10] M. I. Ullah, S. A. Ajwad, M. Irfan, J. Iqbal, "MPC and H-infinity based feedback control of non-linear robotic manipulator", *IEEE International Conference on Frontiers of Information Technology*, Islamabad, Pakistan, December 19-21, 2016
- [11] A. Bemporad, "Model predictive control design: New trends and tools", *IEEE Conference on Decision and Control*, San Diego, USA, December 13-15, 2006
- [12] J. de la Casa Cardenas, A. S. Garcia, S. S. Martinez, J. G. Garcia, J. G. Ortega, "Model predictive position/force control of an anthropomorphic robotic arm", *IEEE International Conference on Industrial Technology*, Seville, Spain, March 17-19, 2015
- [13] H. Ayala, R. Sampaio, D. M. Munoz, C. Llanos, L. Coelho, R. Jacobi, "Nonlinear model predictive control hardware implementation with custom-precision floating point operations", *24th IEEE Mediterranean Conference on Control and Automation*, Athens, Greece, June 21-24, 2016
- [14] M. Makarov, M. Grossard, P. Rodriguez-Ayerbe, D. Dumur, "Generalized predictive control of an anthropomorphic robot arm for trajectory tracking", *IEEE/ASME International Conference on Advanced Intelligent Mechatronics*, Budapest, Hungary, July 3-7, 2011
- [15] J. O. Pedro, T. Tshabalala, "Hybrid NNMP/PID control of a two-link flexible manipulator with actuator dynamics", *10th IEEE Asian Control Conference*, Kota Kinabalu, Malaysia, May 31-June 3, 2015
- [16] H. S. Ali, L. Boutat-Baddas, Y. Becis-Aubry, M. Darouach, " H^∞ control of a SCARA robot using polytopic LPV approach", *14th IEEE Mediterranean Conference on Control and Automation*, Ancona, Italy, June 28-30, 2006
- [17] B. Chen, X. Liu, C. Lin, K. Liu, "Robust H^∞ control of Takagi-Sugeno fuzzy systems with state and input time delays", *Fuzzy Sets and Systems*, Vol. 160, No. 4, pp. 403-422, 2009
- [18] J. C. Doyle, K. Glover, P. P. Khargonekar, B. A. Francis, "State-space solutions to standard H_2 and H_∞ control problems", *IEEE Transactions on Automatic Control*, Vol. 34, No. 8, pp. 831-847, 1989
- [19] M. Makarov, M. Grossard, P. Rodriguez-Ayerbe, D. Dumur, "Modeling and Preview H^∞ control design for motion control of elastic-joint robots with uncertainties", *IEEE Transactions on Industrial Electronics*, Vol. 63, No. 10, pp. 6429-6438, 2016
- [20] S. Manzoor, R. U. Islam, A. Khalid, A. Samad, J. Iqbal, "An open-source multi-DOF articulated robotic educational platform for autonomous object manipulation", *Robotics and Computer-Integrated Manufacturing*, Vol. 30, No. 3, pp. 351-362, 2014
- [21] B. A. Francis, *A Course in H^∞ Control Theory*, Lecture Notes in Control and Information Sciences, Springer-Verlag, 1987

AUTHOR PROFILE



J. Iqbal holds a PhD in Robotics from the Italian Institute of Technology (IIT), Italy and three Master degrees in various fields of Engineering from Finland, Sweden and Pakistan. He is currently working as an Associate Professor in the University of Jeddah, Saudi Arabia. With more than 15 years of multi-disciplinary experience, his research interests include robot analysis and control. He has more than 50 ISI-indexed journal papers on his credit with an H-index of 24. He is a senior member of IEEE, USA.